Averaging for Solitons with Nonlinearity Management

D. E. Pelinovsky,[1] P. G. Kevrekidis,[2] and D. J. Frantzeskakis[3]
[1]*Department of Mathematics, McMaster University, Hamilton, Ontario, Canada L8S 4K1*
[2]*Department of Mathematics and Statistics, University of Massachusetts, Amherst, Massachusetts 01003-4515, USA*
[3]*Department of Physics, University of Athens, Panepistimiopolis, Zografos, Athens 15784, Greece*
(Received 8 July 2003; published 8 December 2003)

We develop an averaging method for solitons of the nonlinear Schrödinger equation with a periodically varying nonlinearity coefficient, which is used to effectively describe solitons in Bose-Einstein condensates, in the context of the recently proposed technique of Feshbach resonance management. Using the derived local averaged equation, we study matter-wave bright and dark solitons and demonstrate a very good agreement between solutions of the averaged and full equations.

DOI: 10.1103/PhysRevLett.91.240201 PACS numbers: 02.30.Jr, 03.75.Lm

Dispersive nonlinear wave equations are appropriate mathematical models for various nonlinear phenomena in fluid mechanics, optics, plasmas, and condensed matter physics. The equation that generically emerges in the description of envelope waves is the nonlinear Schrödinger (NLS) equation [1–3] of the form

$$iu_t = -D\Delta u + \Gamma|u|^2u + V(\mathbf{x})u. \tag{1}$$

Here $u(\mathbf{x}, t)$ is a complex envelope field, $V(\mathbf{x})$ is an external potential, Δ is the Laplacian operator in multidimensions, and D and Γ are the coefficients of the dispersive and nonlinear terms, respectively.

In a number of physical applications, the coefficients D and Γ exhibit temporal periodic variations. When $D = D(t)$, the NLS equation (1) describes the dispersion management (DM) scheme in fiber optics, which is based on periodic alternation of fibers with opposite signs of the group-velocity dispersion. The DM scheme supports robust breathing solitons [4], which are well described through the averaging method by the integral NLS equation [5]. Extensions of the averaging method were developed for *strong* management with large variations of the dispersion coefficient [6] and for *weak* management with small variations of the dispersion coefficient [7].

When $\Gamma = \Gamma(t)$, the NLS equation (1) has applications in optics for transverse beam propagation in layered optical media [8], as well as in atomic physics for the Feshbach resonance [9] of the scattering length of interatomic interactions in Bose-Einstein condensates (BECs). The periodic variation of the scattering length by means of an external magnetic field provides an experimentally realizable protocol for the generation of robust matter-wave breathers [10], and for their persistence against collapse in higher dimensions [11,12]. Solitary waves have become a focal point in studies of BEC both theoretically and experimentally [13,14] due to their coherence properties. Hence, nonlinearity management using Feshbach resonance may provide a viable alternative for the generation of coherent nonlinear wave structures.

Given the importance of applications of Eq. (1) with a periodically varying nonlinearity coefficient, we extend the averaging method of [5,6] to solitons with strong nonlinearity management, when the periodic variations of the nonlinearity coefficient are large in amplitude. Comparing with earlier works, we note that the averaged equation for strong DM in [5,6] is *nonlocal*, whereas our averaged equation [see Eq. (10)] for strong nonlinearity management is *local*. Also, our averaging method is more general than the asymptotic expansion method, exploited for weak DM [7] and for weak nonlinearity management [11]. As the averaged equation obtained herein is simple, we find numerically solitary waves of the averaged equation and compare with those of the full problem, showing the excellent agreement between the two.

Derivation of the averaged equation.—We start with Eq. (1) with $D = 1$ and $\Gamma = \Gamma(t)$. The potential $V(x)$ is left arbitrary but we keep in mind that the magnetic and laser trappings relevant to BEC applications impose parabolic and periodic potentials, respectively. Also, we restrict ourselves to one spatial dimension, but generalization of the method to multidimensions is straightforward. The resulting so-called Gross-Pitaevskii (GP) equation [3] describes the "cigar-shaped" BECs and reads

$$iu_t = -u_{xx} + \Gamma(t)|u|^2u + V(x)u, \tag{2}$$

where the nonlinearity coefficient (proportional to the scattering length in the BECs) $\Gamma(t + \epsilon) = \Gamma(t)$ is a smooth, sign-indefinite, periodic function of period ϵ. We assume that the period ϵ of the nonlinearity management is small compared to the characteristic propagation time of nonlinear waves, while the nonlinearity variations are large in amplitude. In this case, we decompose $\Gamma(t)$ into the mean-value part γ_0 and a large fast-varying part γ, as

$$\Gamma(t) = \gamma_0 + \frac{1}{\epsilon}\gamma(\tau), \qquad \tau = \frac{t}{\epsilon}, \tag{3}$$

where $\gamma(\tau + 1) = \gamma(\tau)$ and $\int_0^1 \gamma(\tau)\, d\tau = 0$. Using

$$u(x,t) = v(x,\tau)\exp\left(-i\int_0^\tau \gamma(\tau')|v|^2(x,\tau')\,d\tau'\right), \quad (4)$$

we remove the large fast variations of the nonlinearity coefficient. In the averaging method (see [6] for details), we decompose solutions of the problem with variable coefficients into a slowly varying mean part $w(x,t)$ and a small, fast-varying part $v_1(x,\tau)$:

$$v(x,\tau) = w(x,t) + \epsilon v_1(x,\tau; w(x,t)), \qquad t = \epsilon\tau. \quad (5)$$

The varying part $v_1(x,\tau;w)$ is a periodic function of τ with unit period. To leading order, this condition is satisfied if $w(x,t)$ satisfies the averaged equation:

$$iw_t = -w_{xx} + \gamma_0|w|^2w + V(x)w + 2i\nu_1 w_x|w|^2_x + i\nu_1 w|w|^2_{xx} + \nu_2 w(|w|^2_x)^2, \quad (6)$$

where $\nu_1 = \int_0^1 \nu(\tau)\,d\tau$, $\nu_2 = \int_0^1 \nu^2(\tau)\,d\tau$, and $\nu(\tau) = \int_0^\tau \gamma(\tau')\,d\tau'$. The averaging method is simplified with the gauge transformation,

$$w(x,t) = \psi(x,t)\exp[i\nu_1|\psi|^2(x,t)], \quad (7)$$

which reduces (6) to the following form:

$$i\psi_t - \nu_1\psi|\psi|^2_t = -\psi_{xx} + \gamma_0|\psi|^2\psi + V(x)\psi + \mu\psi(|\psi|^2_x)^2, \quad (8)$$

where $\mu = \nu_2 - \nu_1^2$. Using the balance equation $i|\psi|^2_t = (\bar\psi_x\psi - \bar\psi\psi_x)_x$, which follows from (8), we rewrite the averaged equation in the final form:

$$i\psi_t = -\psi_{xx} + \gamma_0|\psi|^2\psi + V(x)\psi + \mu\psi(|\psi|^2_x)^2 + i\nu_1\psi(\bar\psi\psi_x - \bar\psi_x\psi)_x. \quad (9)$$

The averaged equation (9) is the main result of this Letter. It is seen to be equivalent to the integral averaged equation derived for strong dispersion management in fiber optics [5,6], but it is a local evolution equation. A similar local equation was also derived for weak dispersion management in fiber optics [7], when the last two terms of (9) are small compared to the leading-order NLS equation. We emphasize that Eq. (9) is derived for strong nonlinearity management and it captures all terms in the same, leading order of the averaging method.

Solitons in BECs.—The simplest standing waves of Eq. (9) are obtained through the standard ansatz [1]:

$$\psi(x,t) = \phi(x)e^{i\omega t}, \quad (10)$$

where $\phi(x)$ solves the second-order differential equation:

$$-\phi'' + \omega\phi + V(x)\phi + \gamma_0\phi^3 + 4\mu(\phi')^2\phi^3 = 0. \quad (11)$$

As a typical example of a smooth periodic variation of the scattering length [11,12], we use the sinusoidal function $\Gamma(t) = \gamma_0 + \gamma_1\sin(2\pi t)$, in which case $\mu = \gamma_1^2/(8\pi^2)$. We also set $\epsilon = 1$ and choose $|\omega| \in [0.1, 0.5]$ to ensure validity of Eq. (11), when $\epsilon \ll 2\pi/|\omega|$. We also use the parabolic potential $V(x)$ for the magnetic trapping of the BEC, $V(x) = \frac{1}{2}\Omega^2x^2$, where $\Omega^2 \in [0.02, 0.4]$.

To estimate actual physical quantities corresponding to the above values of the normalized parameters, we first note that the cases $\gamma_0 < 0$ ($\gamma_0 > 0$) are relevant to an attractive (repulsive) BEC, such as ^{7}Li (^{85}Rb), characterized by a negative (positive) scattering length $a = -1$ nm ($a = 0.8$ nm), in a magnetic field $B \approx 650$ G ($B \approx 159$ G). These values of the scattering lengths set the units in the parameters γ_0 and γ_1, which may take different values as long as the magnetic field B is varied [9]. The number of atoms N in the two BECs is $N = 10^4$ ($N = 2\times10^5$) for $\Omega^2 = 0.4$ ($\Omega^2 = 0.02$) for the ^{7}Li condensate, and $N = 4\times10^3$ ($N = 7.5\times10^4$) for $\Omega^2 = 0.4$ ($\Omega^2 = 0.02$) for the ^{85}Rb condensate. Since we deal with cigar-shaped BECs, the magnetic trap is highly anisotropic, characterized by the confining frequencies $\omega_\parallel = 2\pi\times3.6$ Hz and $\omega_\perp = 2\pi\times360$ Hz in the axial and transverse directions, respectively. Thus, the time and space units in the results that follow are 44.2 ms and 2 μm (for ^{7}Li) or 44.2 ms and 0.6 μm (for ^{85}Rb).

Numerical results.—Using Eq. (11), we can now obtain the solution $\phi(x)$ for a given set of parameters $(\gamma_0, \gamma_1, \Omega, \omega)$, by means of the Newton method. We also

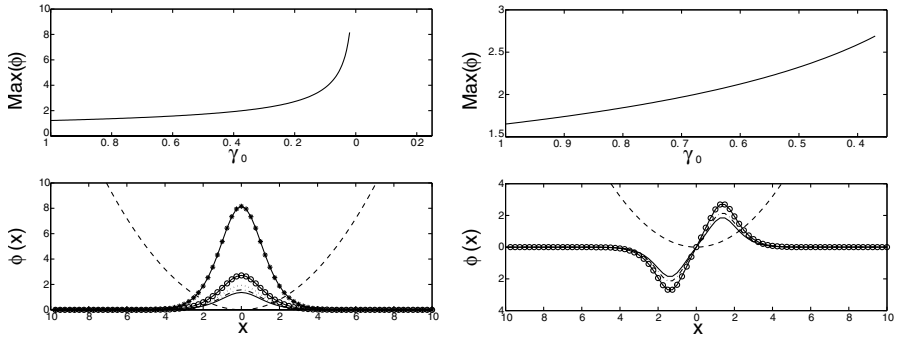

FIG. 1. Bright solitons (left) and twisted solitons (right) of Eq. (11) with $\gamma_0 < 0$, $\gamma_1 = 0.5$, $\Omega^2 = 0.4$, and $\omega = 0.5$. The top subplot shows the solution maximum for different values of γ_0. The bottom subplot shows the potential (dashed line) and the solutions: The left panel shows the solution for $\gamma_0 = -0.8$ (solid line), -0.6 (dash-dotted line), -0.4 (dotted line) -0.2 (circles), and -0.02 (stars), and the right panel for $\gamma_0 = -0.8$ (solid line), -0.6 (dash-dotted line), and -0.37 (circles).

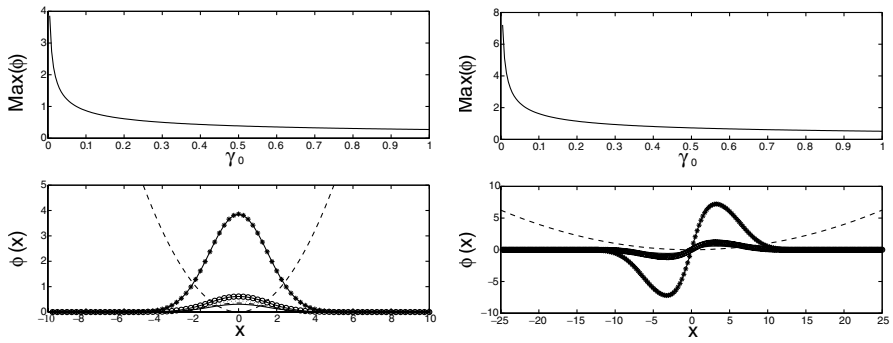

FIG. 2. Same as Fig. 1 but for Thomas-Fermi clouds (left) and dark solitons (right) obtained from Eq. (11) with $\gamma_0 > 0$, $\gamma_1 = 0.5$, $\omega = 0.5$, while $\Omega^2 = 0.4$ (left) and $\Omega^2 = 0.02$ (right). The bottom panel shows the potential (dashed line) and the solutions for $\gamma_0 = 0.8$ (solid line), 0.6 (dash-dotted line), 0.4 (dotted line), 0.2 (circles), and 0.01 (stars). Notice that in the case of the dark soliton (right subplot), the solution profiles are practically indistinguishable between $\gamma_0 = 0.8$ and $\gamma_0 = 0.2$.

perform parameter continuations, to follow the solution branches as the parameters vary.

Figure 1 shows two solutions of Eq. (11) with $\gamma_0 < 0$ (the attractive BEC), $\gamma_1 = 0.5$, $\Omega^2 = 0.4$, and $\omega = 0.5$. The solution in the left panel is the bright soliton, which has the form $\phi(x) = (2\omega/\gamma_0)^{1/2}\mathrm{sech}(\omega^{1/2}x)$ when $\gamma_1 = \Omega = 0$. The solution in the right panel is the so-called twisted soliton, which corresponds to a concatenation of two separated bright solitons of opposite parity (see, e.g., [15]). The twisted soliton does not exist when $\gamma_0 < 0$ and $\Omega = 0$. Higher-order solutions with multiple nodes (zeros) may also exist in Eq. (11) with $\gamma_0 < 0$ and $\Omega \neq 0$, in some parameter domains.

Figure 2 shows two solutions of the averaged equation (11) with $\gamma_0 > 0$ (the repulsive BEC), $\gamma_1 = 0.5$, and $\omega = -0.5$. In the case of $\gamma_0 > 0$, the localized solutions of Eq. (11) bifurcate from linear modes trapped by the parabolic potential $V(x)$, such that an infinite number of solitons with multiple nodes (zeros) exists for larger negative values of ω. The solution in the left panel for $\Omega^2 = 0.4$ is the ground state, often approximated by the Thomas-Fermi cloud [10]. The solution in the right panel for $\Omega^2 = 0.02$ is the (embedded in the Thomas-Fermi cloud) dark soliton which, in the case of $\gamma_1 = \Omega = 0$, has the form $\phi(x) = (|\omega|/\gamma_0)^{1/2}\tanh[(|\omega|/2)^{1/2}x]$ when $\gamma_1 = \Omega = 0$. The dark soliton is a localized solution of Eq. (11) with $\gamma_0 > 0$ and $\Omega = 0$. Notice that the regular dark soliton asymptotes to a nonvanishing amplitude when $\Omega = 0$, while it asymptotes to 0 in the presence of the magnetic trap.

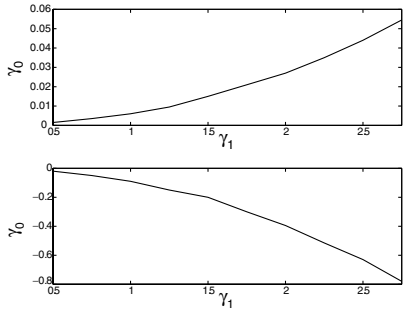

FIG. 3. Domain of existence of dark (top panel for $\Omega^2 = 0.02$) and bright (bottom panel for $\Omega^2 = 0.4$) solitons of Eq. (11) with $|\omega| = 0.5$. The solutions exist above and below, respectively, the corresponding curves of the (γ_1, γ_0) plane.

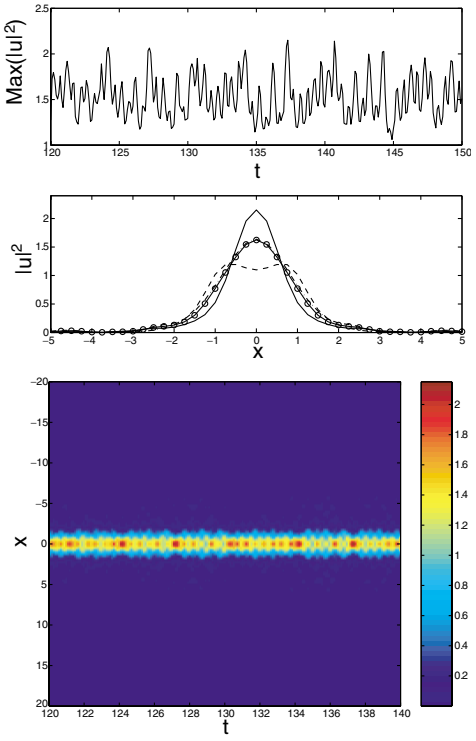

FIG. 4 (color online). Temporal evolution of the bright soliton with $\gamma_0 = -0.5$, $\gamma_1 = 1$, $\Omega^2 = 0.4$, and $\omega = 0.5$. The top panel shows evolution of the (spatial) maximum of $|u(x, t)|^2$ as a function of time. The middle panel shows the solution $|u(x, t)|^2$ at $t = 137.3$ (solid line) and $t = 138$ (dashed line), their average (circles), and the initial configuration (dash-dotted line). The latter practically coincides with the average. The bottom panel shows a contour plot of $|u(x, t)|^2$ in (x, t).

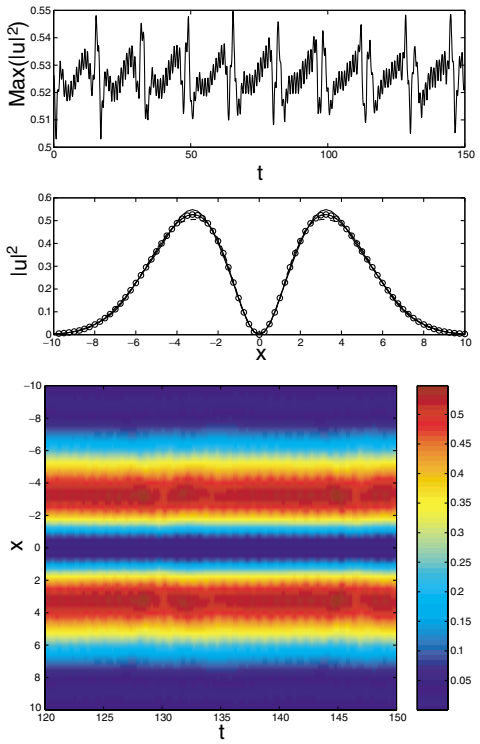

FIG. 5 (color online). Same as Fig. 4, but for the dark soliton with $\gamma_0 = 0.5$, $\gamma_1 = 1$, $\Omega^2 = 0.02$, and $\omega = -0.5$. The maximum and minimum snapshots correspond to $t = 128.4$ and $t = 130.2$. The dash-dotted line of the theoretical prediction (initial condition) again coincides with the average denoted by the circles.

Figure 3 shows two parameter (γ_0, γ_1) continuations of the dark (top panel for $\Omega^2 = 0.02$) and bright (bottom panel for $\Omega^2 = 0.4$) soliton solutions of Eq. (11) with $|\omega| = 0.5$. The branch of dark solitons exists above the bifurcation curve in the top panel, whereas the branch of bright solitons exists below the curve in the bottom panel. The two curves pass through the origin $\gamma_0 = \gamma_1 = 0$. We note that the domain of existence of dark and bright solitons shrinks for increasing values of γ_1.

Finally, we examine how well the averaged Eq. (11) approximates bright and dark solitons of Eq. (2). In our numerical simulations of Eq. (2), we initialize the wave function, using the spatial profile obtained from (11), and then observe whether the temporal evolution of Eq. (2) preserves the average profile of Eq. (11).

Figure 4 shows the temporal evolution of the bright soliton with $\gamma_0 = -0.5$, $\gamma_1 = 1$, $\Omega^2 = 0.4$, and $\omega = 0.5$. The periodic variations of $\Gamma(t)$ in Eq. (2) lead to complicated oscillations of the solution's maximum. While the solution oscillates between single-humped and double-humped solitons (a scenario that bears analogies to the observations of [10]), the average of the two extreme solitons (at the maximum and minimum amplitudes) is practically *indistinguishable* from the profile $\phi(x)$ of Eq. (11).

Figure 5 shows the temporal evolution of the dark soliton with $\gamma_0 = 0.5$, $\gamma_1 = 1$, $\Omega^2 = 0.02$, and $\omega = -0.5$. We notice that the center of the dark soliton remains at the origin $x = 0$, without any oscillations. Only the maxima of $|u|^2(x, t)$ display periodic oscillations of small amplitude. The average of the extreme solitons is again essentially identical to the profile $\phi(x)$ of Eq. (11).

In conclusion, we have derived and studied the averaged equation (9) for the NLS (GP) equation (2) with periodic modulation of the nonlinearity coefficient. Our results are of broad interest to diverse areas of atomic and optical physics, as well as of nonlinear and, also, mathematical physics. We have identified numerically several branches of solitary waves of the averaged stationary equation (11). We have also compared solutions of the averaged and full equations, obtaining a very good agreement.

This work was supported by NSF-DMS-0204585 and the Eppley Foundation.

[1] C. Sulem and P. L. Sulem, *The Nonlinear Schrödinger Equation* (Springer-Verlag, New York, 1999).
[2] Yu. S. Kivshar and G. P. Agrawal, *Optical Solitons From Fibers to Photonic Crystals* (Academic, New York, 2003).
[3] F. Dalfovo *et al.*, Rev. Mod. Phys. **71**, 463 (1999).
[4] S. K. Turitsyn *et al.*, C.R. Phys. **4**, 145 (2003).
[5] I. Gabitov and S. Turitsyn, Opt. Lett. **21**, 327 (1996); JETP Lett. **63**, 861 (1996); M. J. Ablowitz and G. Biondini, Opt. Lett. **23**, 1668 (1998).
[6] D. E. Pelinovsky and V. Zharnitsky, SIAM J. Appl. Math. **63**, 745 (2003).
[7] T. S. Yang and W. L. Kath, Opt. Lett. **22**, 985 (1997); T. I. Lakoba and D. E. Pelinovsky, Chaos **10**, 539 (2000).
[8] I. Towers and B. A. Malomed, J. Opt. Soc. Am. B **19**, 537 (2002); L. Bergé *et al.*, Opt. Lett. **25**, 1037 (2000).
[9] S. Inouye *et al.*, Nature (London) **392**, 151 (1998); E. A. Donley *et al.*, Nature (London) **412**, 295 (2001).
[10] P. G. Kevrekidis *et al.*, Phys. Rev. Lett. **90**, 230401 (2003).
[11] F. Kh. Abdullaev *et al.*, Phys. Rev. Lett. **90**, 230402 (2003); F. Kh. Abdullaev *et al.*, Phys. Rev. A **67**, 013605 (2003); F. Kh. Abdullaev *et al.*, cond-mat/0306281.
[12] H. Saito and M. Ueda, Phys. Rev. Lett. **90**, 040403 (2003).
[13] S. Burger *et al.*, Phys. Rev. Lett. **83**, 5198 (1999); J. Denschlag *et al.*, Science **287**, 97 (2000); K. E. Strecker *et al.*, Nature (London) **417**, 150 (2002); L. Khaykovich *et al.*, Science **296**, 1290 (2002).
[14] V. M. Pérez-García *et al.*, Phys. Rev. A **57**, 3837 (1998); L. Salasnich *et al.*, Phys. Rev. A **65**, 043614 (2002); Y. B. Band *et al.*, Phys. Rev. A **67**, 023602 (2003).
[15] P. G. Kevrekidis *et al.*, New J. Phys. **5**, 64 (2003).